ABOUT THE IMPORTANCE OF RADIATIVE COOLING IN ELECTRONIC PACKAGING

Alejo SÁNCHEZ A*, Rafael ROSALES*, Iris JIMÉNEZ de P*, and Antonio CAMPO**
*Escuela de Ingeniería Mecánica
Universidad de los Andes
Mérida, Edo. Mérida 5101, Venezuela
**College of Engineering
Idaho State University
Pocatello, Idaho, U.S.A

ABSTRACT. Convective cooling has received, so far, more attention than any other cooling mechanism that could be associated with the problem of electronic packaging. This is particularly interesting since the few publications where radiation has been considered show, consistently, that radiative cooling could account for 30-50 % of the total heat transfer.

In the present paper, the Discrete Ordinates method is combined with a control volume approach to simulate the thermal performance of several arrays of electronic components in situations selected to emphasize the importance of the radiation effect. The simulations include radiation combined with pure natural and pure forced convection, as well as radiation combined with mixed convection. In particular, it is demonstrated that in some applications radiation cooling can be orders of magnitude higher than convection cooling. Simultaneously, it is demonstrated that the maximum temperature of electronic components can not be correctly estimated if radiation effects are not accounted for.

1. INTRODUCTION

The trend in the development of more powerful and more compact electronic equipment has resulted in the need for new and better cooling techniques. Of paramount importance in the development of these techniques are the predictions, based on numerical simulations, of the heat transfer mechanisms associated with the electronic components of the equipment.

A review of the pertinent literature shows that convective effects have received more attention than any other mechanism associated with the problem of electronic packaging[1-8]. On the other hand, work considering pure radiation or combined radiation/convection effects is, by far, less common[9-14]. This disparity of attention seems unjustified since the few publications where radiation has been considered show, consistently, that radiative cooling could account for 30-50 % of the total heat transfer and that the maximum temperature of the electronics components can not be accurately predicted if the radiative transfer mechanism is not accounted for.[12-14]

In the present work, a numerical model allowing for the solution of the conjugated problem is presented. Next, the model is implemented for three particular 2-D configurations related to the problem of electronic cooling. The results from these numerical experiments, presented in the form of Nusselt numbers, streamlines, isotherms, and maximum temperature in the component, emphasize the relative importance of radiation cooling in this type of problems. It is also shown in the results that the maximum temperature of the electronic components is consistently overestimated when radiation is ignored.

2. DESCRIPTION OF THE MODEL

2.1 Geometry

Fig. 1 shows two possible setups for electronic components. In the configuration shown in Fig. 1a, the heat dissipating elements are mounted on a board and separated from the rest of the equipment by an upper wall,creating a passage where the cooling fluid circulates. In Fig. 1b, on the other hand, electronic boards or components are placed in a cavity that is characterized by an upper moving wall used to represent the cooling fluid. The heat transfer from the components to the surroundings takes place by convection to the cooling medium, by conduction to the mounting board, and by radiation exchange between all the surfaces.

2.2 Governing Equations

The model to be used in this work has been extensively applied to the solution of problems in 1-, 2- and 3-D and for both participating and transparent media[10-15]. However, the formulation to be presented next will be restricted to 2-D and no-participating medium since this is the type of problem to be solved here.

For laminar flow and steady-state conditions, with all the properties of the fluid assumed constant except for the density related to the buoyancy effect, (Boussinesq approximation in the y momentum equation), the transport equations for 2-D flow are:

Continuity:

$$\frac{\partial}{\partial \xi}\left(\bar{u}\right) + \frac{\partial}{\partial \eta}\left(\bar{v}\right) = 0 \qquad (1)$$

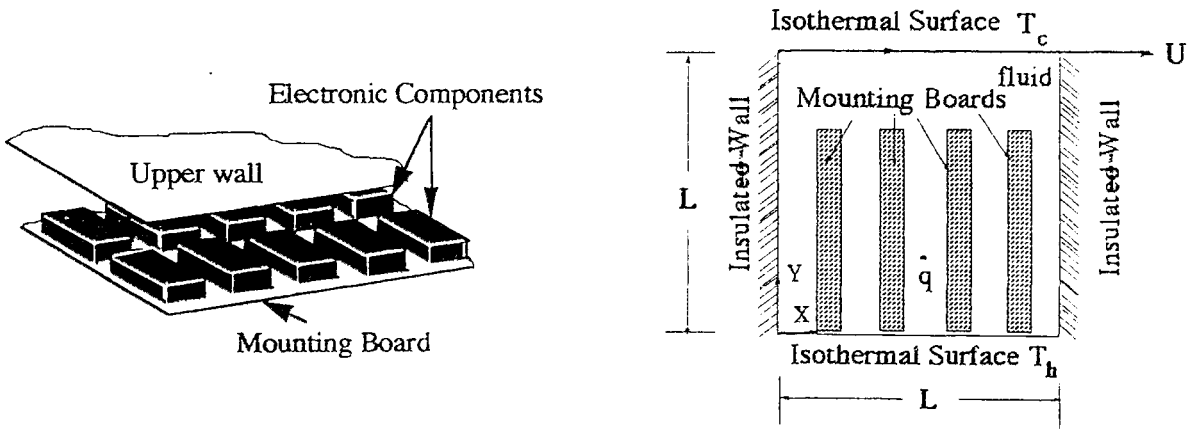

Figure 1. Schematic diagram of general geometry

x-momentum:

$$\frac{\partial}{\partial\xi}\left(\bar{u}\ \bar{u}\right)+\frac{\partial}{\partial\eta}\left(\bar{u}\ \bar{v}\right)=\mathrm{Pr}\left[\frac{\partial}{\partial\xi}\left(\frac{\partial\bar{u}}{\partial\xi}\right)+\frac{\partial}{\partial\eta}\left(\frac{\partial\bar{u}}{\partial\eta}\right)\right]-\frac{\partial\bar{P}}{\partial\xi} \tag{2}$$

y-momentum:

$$\frac{\partial}{\partial\xi}\left(\bar{v}\ \bar{u}\right)+\frac{\partial}{\partial\eta}\left(\bar{v}\ \bar{v}\right)=\mathrm{Pr}\left[\frac{\partial}{\partial\xi}\left(\frac{\partial\bar{v}}{\partial\xi}\right)+\frac{\partial}{\partial\eta}\left(\frac{\partial\bar{v}}{\partial\eta}\right)\right]-\frac{\partial\bar{P}}{\partial\eta}+\mathrm{Ra}\,\mathrm{Pr}\,\theta \tag{3}$$

energy:

$$\frac{\partial}{\partial\xi}\left(\bar{u}\ \theta\right)+\frac{\partial}{\partial\eta}\left(\bar{v}\ \theta\right)=\frac{\partial}{\partial\xi}\left(\frac{\partial\theta}{\partial\xi}\right)+\frac{\partial}{\partial\eta}\left(\frac{\partial\theta}{\partial\eta}\right)+\bar{Q}-\nabla\bar{q}_r \tag{4}$$

In the previous equations, ξ and η are dimensionless distances in the x and y directions respectively; velocities are normalized with α/L and the pressure is normalized with $\rho\ \alpha^2/L^2$; θ represents $(T - T_C)/(T_h - T_C)$; Pr y Ra are the Prandtl and Rayleigh numbers respectively. The fluid properties are taken as ρ for density, α for thermal diffusivity and k_f for thermal conductivity. T is the fluid temperature. Finally, $\bar{Q}$ represents the dimensionless heat generation defined as $\dot{q}\ L^2/k_f(T_h - T_C)$ where $\dot{q}$ is known in the electronic component, and zero everywhere else in the numerical domain.

The boundary conditions for Eq. 1-4 will be specified for each problem later.

2.3 Radiation Fluxes

The propagation of radiation (I) along a line-of-sight direction ζ is described by the radiative transfer equation. Without scattering or absorption, the change in the radiant intensity $I(\zeta)$ in the $\bar{\omega}$-direction is expressed by

$$\frac{dI}{d\zeta}=0 \tag{5}$$

For black or gray enclosures, Eq. 5 is subjected to the following boundary conditions

$$I^{+}=\varepsilon I_b^{+}+\frac{\rho}{\pi}\int_0^{2\pi}\left(I^{-}(\bar{\omega}_i)\ \eta\ d\omega^{-}\right) \tag{6}$$

In Eq. 6, superscripts + and - indicate radiation going from the boundary toward the medium inside the domain, and from the medium toward the boundary, respectively. The boundary has an emittance ε and blackbody intensity I_b^{+}, which depends on the temperature of the surface. The reflectance of the boundary is denoted by ρ, which, for convenience, is taken to be independent of direction. The cosine of the angle between the direction of propagation of I^{-} and the normal to the given boundary is η. Physically, the terms on the right hand side of Eq.6 represent emission, and diffuse reflection of incident intensity from within the medium. The intensity I_b^{+} is assumed known.

Finally, the net radiative heat flux on a given surface is expressed as

$$q_r = \int_{4\pi} I \; \eta \, d\zeta \tag{7}$$

2.4 Component-Fluid Interface (Internal Boundaries)

The treatment given to the component-fluid interface requires particular attention. This interface is shown in Fig. 2 where two adjacent control volumes, one in the solid component and the other in the contiguous fluid, are represented. T_f and T_s are the average temperature, for the control volumes corresponding to the fluid and the solid side respectively, and δ_f y δ_s are the corresponding distances from center to boundary. q_r is the net radiative flux leaving the component through the specified control volume.

An energy balance at the boundary indicates that the temperature of the interface (needed by the radiative model) can be written as

$$T_i = \frac{\frac{k_s}{\delta_s} T_s + \frac{k_f}{\delta_f} T_f - q_r}{\frac{k_s}{\delta_s} + \frac{k_f}{\delta_f}} \tag{8}$$

where k_s and k_f are the thermal conductivities for the solid and the fluid, respectively.

Similarly, an energy balance on the control volume situated in the solid side indicates that Eq. 4 should be modified for these interface-control-volumes, substituting $\bar{Q}$ by

$$\bar{Q} - \bar{q}_r \tag{9}$$

where

$$\bar{q}_r = \frac{q_r \, L}{k_f (T_h - T_c)} \tag{10}$$

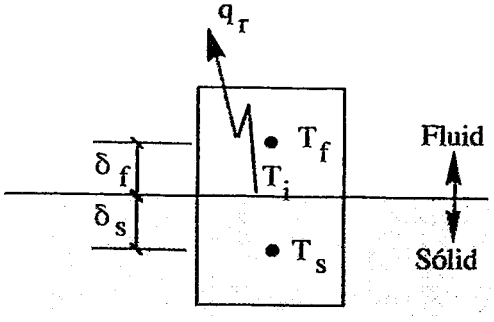

Figure 2. Interface component-fluid

2.5 Nusselt Numbers and Energy Balance

At the hot or cold wall , the convective Nusselt numbers (Nu_h and Nu_c respectively) were evaluated as[15]

$$Nu_{h \text{ or } c} = - \frac{q''(h \text{ or } c)\, L}{k_f\,(T_h - T_c)} = - \int_0^1 \left. \frac{\partial \theta}{\partial \eta} \right|_{\eta=0} d\xi \qquad (11)$$

where $\bar{q}''$ is the average heat flux per unit area, due to convection alone, on the wall being considered. It should be noticed that Eq. 11 is equally used in regions where the component or the fluid is present. In the former case, therefore, an equivalent "conductive" Nusselt is being defined.

Similarly, the Nusselt numbers due to radiation are defined as

$$Nu_{rh \text{ or } rc} = - \frac{q''r(h \text{ or } c)\, L}{k_f\,(T_h - T_c)} \qquad (12)$$

In order to check for the conservation of energy, an energy balance (E) will be performed as

$$E = \frac{|q'_{net}| \times 100}{q'_{in} + \dot{q}\, Lx\, Ly} \qquad (13)$$

where

$$q'_{net} = q'_{in} + q'_{out} + \dot{q}\, Lx\, Ly \qquad (14)$$

In Eq. 11-14, subscripts h, c, and r indicate hot wall, cold wall, and radiation respectively; k_f is the thermal conductivity of the fluid; superscripts " and ' indicate per unit area, and per unit length respectively; q is the heat flux; and Lx and Ly are the x and y dimensions of the heat generating source.

3. NUMERICAL PROCEDURE

Before commenting on the results obtained in the three experiments performed in this work, a few general comments on the numerical procedure are needed.

The governing equations were solved by means of a control volume approach and the SIMPLER algorithm[16]. This model was coupled with a discrete ordinates algorithm to solve for the radiative transfer equation. Following recommendations from other studies related to radiative transport in transparent media[17], the discrete ordinates algorithm was implemented with an equally spaced, equally weighted quadrature set and a finite-difference factor of 0.6.

When the working fluid is a nonparticipating medium, the transport equations and the radiative transfer equation are explicitly decoupled. Their solution, however, is implicitly interdependent through the boundary conditions.

Convergency problems have already been reported for the type of geometry used in Experiments 2 and 3 and shown in Fig. 1b (in the absence of radiation[7,8]), and similar limitations have been reported in

partitioned cavities without moving boundary or heat generation (with radiation[18], and without it[19]). Steady state conditions (when they exist) are reached after a long period of instability that requires low underrelaxation factors and, consequently, hundreds and even thousands of iterations.

Based on the sensitivity analysis for the grid reported in[20], it was decided to use an uniform 42x42 grid mesh for Experiments 2 and 3. However, due to the presence of heat generating protrusions and the instability problem reported above, a finer, non-uniform grid seems advisable. For the preliminary results reported here, it was not considered necessary to further increase the computational effort and the 42x42 uniform grid mesh was maintained. Even with this limitation, an average wall clock time of two minutes per convection-radiation-iteration and 30 seconds for a pure-convection-iteration was needed on a personal computer, with a typical experiment –changing only one parameter– requiring about 1500 iterations starting from a previously converged, related, problem. For Experiment 1, a 32x22 grid mesh was considered to be sufficient.

A given experiment was considered converged when none of the variables changed, between successive iterations, in more than $1x10^{-4}$ and the summation of the residual mass was less than $1x10^{-5}$. Depending on the experiment, the relaxation factor needed values between 0.1 and 0.6.

4. EXPERIMENTS AND RESULTS

Three different experiments, related to the problem of electronic cooling, were performed:

4.1 Experiment 1: Infinite Channel

A particular case of the general geometry presented in Fig. 1a is the 2-D configuration shown in Fig. 3.

In this configuration, the working fluid (air) enters the channel with a mean velocity U (taken as reference velocity) and uniform temperature T_c (reference temperature). The electronic setup has a periodicity 3H and, as a consequence, the numerical domain is reduced to that shown in Fig. 3. The upper and lower plates are maintained at a uniform and constant temperature T_h. All surfaces are considered to be black and the electronic components have the dimensions indicated in the figure and generate heat at a rate $\dot{q}$ (w/m^3).

Several tests were performed in this experiment. In all cases, the dimensions of the components remained constant. Also constant were the parameters $k_f = 0.03$, $k_s/k_f = 10$, $Pr = 1$, $Ra = 0.0$, $T_h = 200$ K, $T_c = 0$ K, $L/H = 3$. The Reynolds number was varied from 10 to 200 and the dimensionless heat generation ($\bar{Q}$) took values of 500 and 1000.

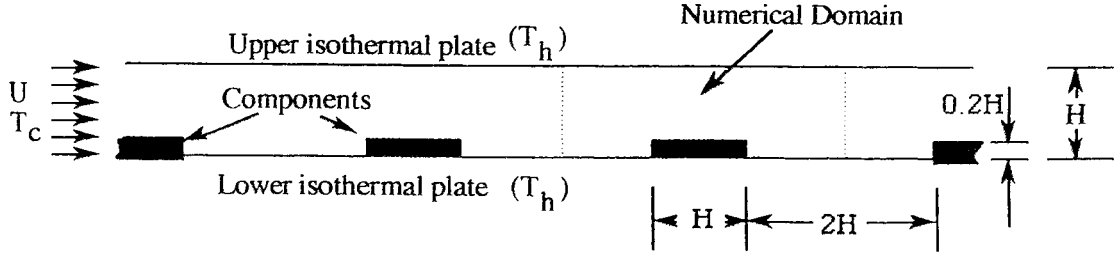

Figure 3. Geometry for Experiment 1

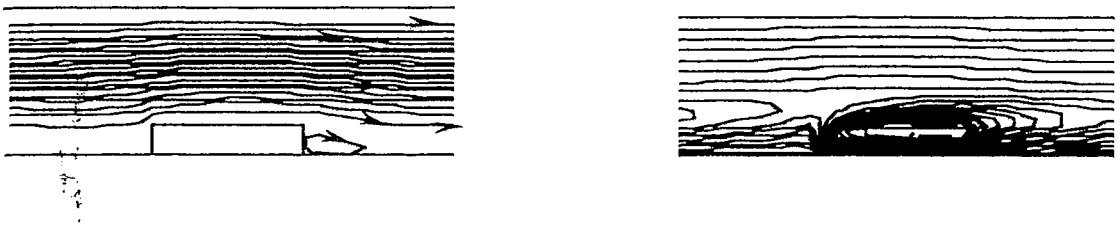

(a) (b)

Figure 4. (a) 20 Equally spaced streamlines ; (b) 20 Equally spaced isotherms $\theta_{max} = 2.86$ in * ; (Re = 100, $\bar{Q} = 1000$, (without radiation)

Fig.4 shows the streamlines (a) and the isotherms (b) corresponding to the test with Re = 100 and $\bar{Q}$ = 1000. The periodicity of the boundary conditions can easily be seen in the figure.

The isotherm and streamline distributions for the other tests are very similar to those shown in Fig. 4 and will not be presented here. Of greater interest for this study are the numerical results of Nusselt numbers and maximum temperatures obtained in the different tests. These results are presented in Table 1 where Nu_l and Nu_u are the Nusselt numbers due to convection on the lower and upper plates respectively (Eq. 11); Nu_{rl} and Nu_{ru} are the corresponding Nusselt numbers due to radiation (Eq. 12); $\%q_k$ is the percentage of the total heat loss due to conduction through the base of the component; and finally, θ_{max} is the maximum temperature of the component.

Table 1

Summary of Nusselt numbers, θ_{max} and $\%q_k$ for Experiment 1

Re	$\bar{Q}$	Radiation?	Nu_l	Nu_u	Nu_{rl}	Nu_{ru}	$\%q_k$	θ_{max}
10	500	No	1.02	0.534	—	—	95.3	1.96
		yes	0.927	0.485	0.056	1.65	90.6	1.87
	1000	No	2.05	1.07	—	—	95.3	2.91
		yes	1.69	0.879	0.192	6.21	84.4	2.58
100	500	No	1.58	0.569	—	—	93.6	1.93
		yes	1.45	0.561	0.053	1.55	89.1	1.85
	1000	No	3.17	1.17	—	—	93.5	2.86
		yes	2.66	1.03	0.182	5.86	85.3	2.55
200	500	No	1.73	0.628	—	—	92.9	1.92
		yes	1.59	0.617	0.052	1.52	88.6	1.84
	1000	No	3.48	1.29	—	—	92.8	2.84
		yes	2.92	1.14	0.179	5.75	84.9	2.54

In this problem the component, with a thermal conductivity that is 10 times larger than that of the surrounding fluid, is mounted on a board that has no thermal resistance. As a consequence of this, more than 80% of the cooling effect takes place by conduction through the bottom of the component and less

than 16% is due to the combined convection-radiation mechanisms. Of particular importance for this study is the finding that the contribution of radiation to this combined radiation-convection cooling, ranges from 14% (for $\bar{Q} = 500$) to 40% (for $\bar{Q} = 1000$). Furthermore, it can be easily verified in Table 1 that when radiation is not considered, the maximum temperature of the components is always overpredicted. This overprediction ranges from 4% (for $\bar{Q} = 500$) to 12% (for $\bar{Q} = 1000$).

4.2 Experiment 2: Lid Driven Cavity with Vertical Heat Generating Partitions

A particular case of the general geometry presented in Fig. 1b, is the configuration shown in Fig. 5a. In this configuration, a single board of dimensions 0.095L x 0.38L and dimensionless heat generation $\bar{Q}$ = 1000 is placed at the center of a square cavity with the upper wall of the cavity having a velocity U (taken as reference). The following parameters are maintained fixed during the experiment: $k_f = 0.03$, k_s/k_f = 10, Pr = 1, Ra = 0.0, Re = 100, T_h = 300 K, $T_c = 0.9T_H$ K (T_c is taken as reference temperature).

Fig. 5b shows exponentially separated streamlines while Fig. 5c shows equally spaced isotherms. Also indicated in Fig. 5b is the location (point x) where the maximum stream function (ψ_{max} = -.0877589) takes place. Similarly, the location of maximum temperature (θ_{max} = 1.0653594 at location x) is shown in Fig. 5c.

The following results were obtained: Nu_u= -3.56, Nul = 1.31, Nu_{ru} = -114.8, Nu_{ru} = 77.65; the equivalent Nusselt number due to conduction through the base of the board is -1.28; energy was conserved within 0.5% according to Eq. 13. It can be deduced from these results that, for this particular experiment, radiation accounts for more than 96% of the combined radiation-convection cooling effect.

4.3 Experiment 3: Lid Driven Cavity with Horizontal Heat Generating Protrusions

Several tests were performed on the same geometry of the previous experiment but with the protrusion (of dimensions 0.38L x 0.095L) placed horizontally and centered on the base plate. For these experiments: T_h = 300 K and T_c = 200 K. All the other parameters were the same as those in the previous experiment.

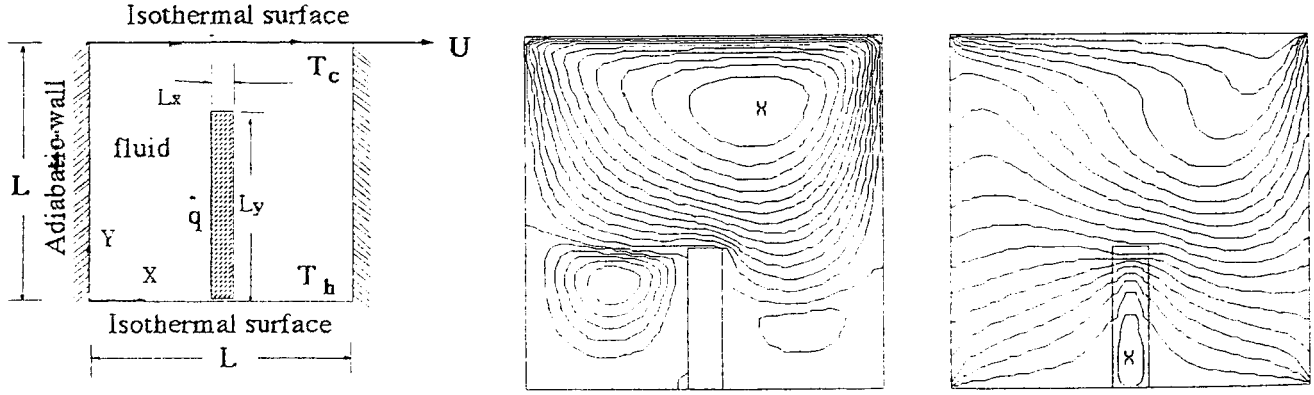

(a) (b) (c)

Figure 5. (a) Geometry for experiment 2 ; (b) Streamlines; (c) Isotherms

Table 2 shows the results obtained in the different tests. It can be noticed that the test included pure natural and pure forced convection, as well as mixed convection. Of particular interest for this study is the fact, shown in Table 2, that when radiation is not included in the modeling, the maximum temperatures of the chip are strongly overpredicted. This can be easily corroborated by noticing that the maximum temperature predicted for pure convection, with a dimensionless heat generation of 200, was 1.0709. This value represents a 7% overprediction when compared with the maximum temperature obtained, for the same problem, when radiation is included. Further, this value is still around 3% higher than the maximum temperature obtained, including radiation, when the heat generation is raised to 1000 (five times more).

Table 2 also shows that, in all the tests performed, radiation accounted for more than 86% of the combined radiation-convection cooling effect.

Table 2

Summary of Nusselt numbers, θ_{max}, $\bar{Q}$, and Gr/Re^2 for Experiment 3

Radiation?	Gr/Re^2	$\bar{Q}$	Nu_l	Nu_u	Nu_{rl}	Nu_{ru}	Energy Balance Equation (13)	θ_{max}
No	0.0	0.0	2.08	-2.02	–	–	2.89%	1.0
		200	-5.75	-2.13	–	–	1.43%	1.0709
Yes	0.0	0.0	18.63	-3.62	48.59	-64.64	1.55%	1.0
		200	13.44	-3.73	47.83	-66.63	1.576%	1.0
		500	5.77	-3.85	46.69	-69.67	1.46%	1.0
		1000	-6.83	-4.11	44.74	-74.95	1.33%	1.0399
Yes	0.1	1000	-6.83	-4.26	44.74	-74.95	1.51%	1.0399581
Yes	1.0	1000	-6.79	-4.43	44.75	-74.92	1.61%	1.0395
Yes	10.0	1000	-6.06	-5.48	44.97	-74.32	1.02%	1.0354

5. CONCLUSIONS

In the present work, a numerical model allowing for the solution of the conjugated problem was presented. Next, the model was implemented for three particular 2-D configurations related to the problem of electronic cooling. The results from these numerical experiments, presented in the form of Nusselt numbers, streamlines, isotherms, and maximum temperature in the component, emphasize the importance of radiation cooling in this type of problems. In particular, it was shown that, for the experiments presented here, radiation cooling ranges from 14% to more than 96% of the total radiation-convection cooling effect, even for low working temperatures.

It was also shown that the maximum temperature of the electronic components is consistently overestimated when radiation is ignored. For the experiments performed here, this overprediction ranged from 4% to 12%.

Based on the results obtained here, and considering previous experiences from these and other authors, it can be concluded that modeling the cooling of electronic devices as pure convection is seldom justifiable.

Radiation modeling should. therefore, be included in all numerical simulations related to electronic cooling.

6. REFERENCES

1. Sparrow, E. M., Niethammer, J. E., and Chaboki, A., Heat Transfer and Pressure Drop Characteristics of Rectangular Modules Encountered in Electronic Equipment, Int. J. Heat and Mass Transfer, Vol. 25, No. 7, pp. 961-973, 1982.

2. Braaten, M. E. and Patankar, S. V., Analysis of Laminar Mixed Convection in Shrouded Arrays of Heated Rectangular Blocks, Int. J. Heat and Mass Transfer, Vol. 28, No. 9, pp. 1699-1709, 1985.

3. JWang, X., Robillard, L., and Vasseur, P., Laminar Mixed Convection Heat Transfer Between Parallel Plates with Periodically Localized Heat Sources, Eds. A. Ortega, D. Agonafer, and B. W. Webb, Heat Transfer in Electronic Equipment, HTD-Vol. 171, A.S.M.E., pp. 81-87, 1991.

4. Asako, Y. and Faghri, M., Three-Dimensional Heat Transfer in a Fluid Flow Analysis of Arrays of Square Blocks Encountered in Electronic Equipment, J. Num. Heat Transfer,, Vol. 13, pp. 481-498, 1988.

5. Afrid, M. and Zebib, A., Natural Convection Air Cooling of Heated Components Mounted on a Vertical Wall, J. Num. Heat Transfer,, Part A, Vol. 15, pp. 243-259, 1989.

6. Shaw, H. J., Chen, W. L., and Chen, C. K., Study of the Laminar Mixed Convective Heat Transfer in Three-Dimensional Channel with a Thermal Source, J. of Electronic Packaging, Vol. 113, pp. 40-49, 1991.

7. Papanicolaou, E. and Jaluria, Y., Mixed Convection from an Isolated Heat Source in a Rectangular Enclosure, J. Num. Heat Transfer, Part A, Vol. 18, pp. 427-461, 1990.

8. Papanicolaou, E. and Jaluria, Y., Mixed Convection from Simulated Electronic Components at Varying Relative Positions in a Cavity, J Heat Transfer, Vol. 116, pp. 960-970, 1994.

9. Lee, S. and Yovanovich, M. M., Conjugate Heat Transfer from a Vertical Plate With Discrete Heat Sources under Natural Convection, ASME paper No. 89-WA/EEP-9, 1989.

10. Smith, T. F., Beckermann, C., and Weber, S. W., Combined Conduction, Natural Convection, and Radiation Heat Transfer in an Electronic Chassis, J. of Electronic Packaging, Vol. 113, pp. 382-391, 1991.

11. Bravo, R. H., Sánchez, A., Chen, C. J., and Smith, T. F., Convection and Radiation Heat Transfer Analysis in Three-Dimensional Arrays of Electronic Chips, Proc. of the 1992 IEEE Inter Society Conference on Thermal Phenomena in Electronic Systems, Austin, pp. 149-154, 1992.

12. Hawkins, L. E. and Nelson, D. J., A Design Methodology for Vertical Channel Flow and Heat Transfer, Proc. of the 1992 IEEE Inter Society Conference on Thermal Phenomena in Electronic Systems, Austin, pp. 15-22, 1992.

13. Sánchez, A., Bravo, R., and Smith, T. F., Surface Radiation Exchange in Multi–Dimensional Arrays of Electronic Components, 6th International Symposium on Transport Phenomena (ISTP–6) in Thermal Engineering, Vol. 1, pp.267-272, Seoul, Korea, 1993.

14. Beckermann, C., Smith, T. F., and Pospichal, B., Use of a Two-Dimensional Simulation Model in the Thermal Analysis of a Multi-Board Electronic Module, J. of Electronic Packaging, Vol. 116, pp. 126-133, 1994.

15. Sánchez, A., Krajewski, W. F., and Smith, T. F., A General Purpose Radiative Transfer Model for Application to Remote Sensing in Multi-Dimensional Systems, IIHR Report No. 355, Iowa Institute of Hydraulic Research, The University of Iowa, Iowa City, Iowa, 1992.

16. Patankar, S. V., Numerical Heat Transfer and Fluid Flow, McGraw-Hill, New York, 1980.

17. Sánchez, A. and Smith, T. F., Surface Radiation Exchange for Two-Dimensional Rectangular Enclosures Using the Discrete-Ordinates Method, J Heat Transfer, Vol. 114, No. 2, pp. 465-472, 1992.

18. Yucel, A. and Acharya, S., Natural Convection of a Radiating Fluid in a Partially Divided Square Enclosure, Eds. S. T. Thynell and J. R. Mahan, Radiation Heat Transfer, HTD-Vol. 154, A.S.M.E., pp. 19-28, 1990.

19. Chuang, S., Chen, M., and Sun, C., Numerical Study of Natural Convection in a Partitioned Enclosure, Proceedings of the 6th International Symposium on Transport Phenomena in Thermal Engineering, Seoul, Korea, 1993.

20. Sánchez, A., Morales, J. C., and Campo, A., Application of the Discrete Ordinates Method to Buoyancy-Induced Radiating Fluids in a Square Enclosure with a Moving Wall, in General Papers in Radiative Heat Transfer, ASME-HTD, Vol. 257, pp. 25-32, 1993.